Micellar anisometry in lyotropic uniaxial nematic phases studied by transversal NMR relaxation dispersion

C. R. Rodriguez,[1] D. J. Pusiol,[1] A. M. Figueiredo Neto,[2] and C. A. Martin[1]
[1]*Facultad de Matemática, Astronomía y Física, Universidad Nacional de Córdoba, Ciudad Universitária, X5016LAE Córdoba, Argentina*
[2]*Instituto de Física, Universidade de São Paulo, Caixa Postal 66318 05315-970, São Paulo, SP, Brazil*
(Received 5 September 2003; published 30 April 2004)

A new method, based on the measurement of the ^{23}Na nuclei spin-spin NMR relaxation times (T_2), is proposed to investigate the shape of micelles in lyotropic nematic phases. We investigate the ternary lyotropic mixture of sodium dodecyl sulfate, 1-decanol, and water by using the NMR technique, measuring T_2 in the two lyotropic uniaxial nematic phases. The characteristic relaxation time curves of each particular phase are analyzed by considering that they are constituted by a superposition of exponential decays with typical characteristic times: in a sense, a T_2 spectroscopy. The analysis of the T_2 dispersion profiles in both the uniaxial nematic calamitic and discotic phases indicates that our results can be interpreted in terms of the model of intrinsically biaxial micelles in all the nematic phases.

DOI: 10.1103/PhysRevE.69.041708 PACS number(s): 61.30.Eb, 61.30.Gd, 76.60.Gv, 76.60.Es

I. INTRODUCTION

One of the most interesting example of self-assembled system [1] is the micellar lyotropic liquid crystal [2], in particular the lyotropic nematic phases [3–5]. Three types of lyotropic nematic phases were identified: two of them are uniaxial (labeled N_C for calamitic nematic and N_D for diskotic nematic) and the third one is a biaxial phase [4] (labeled N_B).

Regarding the micellar shape, Fujiwara and co-workers [6], proposed that the micelles were cylinders (e.g., prolate ellipsoids) and disks (e.g., oblate ellipsoids) in the N_C and N_D phases, respectively. X-ray diffraction patterns of these phases [3] allowed the determination of the reciprocal space structures of the uniaxial nematics. They were schematized as a torus with its major axis parallel to the director **n**, and an elongated hollow circular cylinder with an axis parallel to **n**, in N_C and N_D phases, respectively. This interpretation is consistent with the picture of cylindric and discotic micelles, *but* these micellar shapes *are not the unique* that could produce the reciprocal space images obtained in the x-ray experiments.

When in 1980 Yu and Saupe [4] identified the N_B phase a question arose: do the micelles change their shape to a biaxial one at the uniaxial-to-biaxial transition or is there a mixture of disks and cylinders in the biaxial phase? Both possibilities account for almost all the experimental results accumulated until now but it is important to note that there is not a direct experimental evidence of the presence of cylinders or disks in lyotropic mixtures which present the three nematic phases. On the other hand, neutron scattering experiments [7] in N_C phases of ternary mixtures (with two amphiphiles) clearly shown that there are no cylinders in this phase, reinforcing the model of intrinsically biaxial micelles (MIBM) proposed by Galerne and co-workers [5]. In this model, it is assumed that there are similar micelles in the three nematic phases. These micelles have a biaxial symmetry (as a flattened prolate ellipsoid, with three symmetry axes of order two, mutually orthogonal) and the three nematic phases are consequence of orientational fluctuations of these micelles. In the case of binary mixtures, where only one (always uniaxial) nematic phase is present, symmetry reasons can be evoked to justify the existence of higher symmetric objects like disks and cylinders but, in mixtures with more than one amphiphile, this argument cannot be straightforward applied. Another important result obtained by means of the neutron scattering experiments in lyotropic nematic ternary mixtures [7] is that the alcohol and the principal amphiphile are not homogeneously distributed in the micelle. The alcohol and the principal amphiphile molecules are located mainly in the flat and curved parts of the micelle, respectively.

Different complementary techniques, e.g., nuclear magnetic resonance (NMR) quadrupole splitting [8], electric conductivity [9,10], x-ray and neutron scattering [5,11,12], and freeze-fracture electron microscopy [13], among others, where used to investigate the structure and local ordering of these lyotropic systems. Nevertheless the MIBM accounts to all the available experimental results (to the best of our knowledge), we believe that complementary experiments to reinforce its basis are useful and necessary.

In the present work we investigate the ternary lyotropic mixture of sodium dodecyl sulfate (SDS), 1-decanol (DeOH), and water by using the NMR technique, measuring the ^{23}Na nuclei spin-spin relaxation times (T_2) in the two lyotropic uniaxial nematic phases. The characteristic relaxation time curves of each particular phase (at a given relative concentrations and temperature conditions) are analyzed by considering that they are constituted by a superposition of exponential decays with typical characteristic times: in a sense, a T_2 spectroscopy. This technique allows the determination of the different T_2 contributions to the NMR signal, each of them associated to a given distance between ^{23}Na nuclei and, consequently, with the micellar curvatures. Multiexponential decay of the transversal magnetization has been observed in other systems, but the explanation proposed here

TABLE I. Samples description in terms of M_ω and M_d (see text for definition) and phase sequence. COA and POL states for coagel phase and polyphasic domain, respectively.

Sample	Phase sequence	$M_\omega(\pm 0.2)$	$M_d(\pm 0.005)$
Binary	$\overset{T\lesssim 290\ \mathrm{K}}{\rightarrow}$ ISO $\overset{T\gtrsim 310\ \mathrm{K}}{\rightarrow}$	44.0	0
NC1	COA $\overset{T\sim 298\ \mathrm{K}}{\rightarrow}$ N_C $\overset{T\sim 304\ \mathrm{K}}{\rightarrow}$ POL	45.2	0.200
NC2	COA $\overset{T\sim 298\ \mathrm{K}}{\rightarrow}$ N_C $\overset{T\sim 306\ \mathrm{K}}{\rightarrow}$ POL	45.2	0.310
NC3	COA $\overset{T\sim 292\ \mathrm{K}}{\rightarrow}$ N_C $\overset{T\sim 296\ \mathrm{K}}{\rightarrow}$ POL	46.5	0.330
ND1	COA $\overset{T\sim 290\ \mathrm{K}}{\rightarrow}$ N_D $\overset{T\sim 296\ \mathrm{K}}{\rightarrow}$ POL	44.8	0.400

is conceptually different. Brownstein and Tarr [14] assumed that classical diffusion of water in the interstitial volume between biological cells is the responsible for the multiexponential decay and claimed that this phenomenon can only be observed in samples whose size is of the order of a biological cell, much larger than the typical micellar sizes investigated in the present study.

II. EXPERIMENT SECTION

A. Sample preparation and methods

Sodium dodecyl sulfate and 1-decanol were Merck supplied. Light water was tridestilated and deionized in our laboratory. The lyotropic mixtures were prepared by weighing the appropriate amounts of components in test tubes and placed in a heated bath (at 30 °C), sonicated and centrifuged until being homogeneous under crossed polarizers. The composition of the samples is expressed in terms of the relative molar ratio M_X of substance X ($X=\omega$, or d for water and 1-decanol, respectively) with respect to the SDS, given by [15]

$$M_X = \left(\frac{\text{wt \% of } X}{\text{wt \% of SDS}}\right)\left(\frac{W_{SDS}}{W_X}\right),$$

where W_{SDS} and W_X are the molecular weights of SDS and X, respectively. All the samples were prepared at $M_\omega \sim 45$. The relative compositions of the mixtures are given in Table I. Changes in the transition temperatures were observed with respect to those reported in Ref. [15]. This fact, common in the field of lyotropics, was attributed to the origin of the mixture components used in our experiment, different from that of Amaral and Helene [15]. The phases identified in this phase diagram are the uniaxial calamitic nematic (N_C), uniaxial discotic nematic (N_D), coagel (COA) and a nematic-isotropic phase coexistence domain (polyphasic domain, referred to here as POL).

B. Technique and apparatus

The NMR apparatus used is a Bruker MSL-300 with a magnet of 7.05 T, and a double bearing CP/MAS probe with 7 mm spinners. The uniformity of the magnetic field along the whole sample volume, achieved by means of conventional shimming coils, is better than 0.01 ppm. The sample temperature was set and controlled over the working range from 298 K to 330 K better than ±0.1 K.

The pulse sequence used to perform the T_2 measurements is the standard CPMG with receiver and pulses phase cycling [16,17]. The general expression for the heteronuclear (with spins I from the proton and $S=3/2$ from the sodium) dipolar transverse relaxation rate for single quantum coherence, in terms of the reduced intensity function and for a given interdipole distance (r) is written as [18]

$$\frac{1}{T_2} = \frac{S(S+1)}{r^6}\left(\frac{\mu_0\,\hbar\,\gamma_I\,\gamma_S}{4\pi}\right)^2\left[\frac{1}{6}\mathcal{J}_0(\omega_I-\omega_S)+\frac{3}{2}\mathcal{J}_1(\omega_I)+\frac{3}{4}\mathcal{J}_2(\omega_I+\omega_S)\right], \tag{1}$$

where μ_0 is the magnetic permeability, γ_I and γ_S are the proton and the sodium gyromagnetic ratios respectively, and $\mathcal{J}_{0,1,2}(\omega)$ are the reduced spectral densities. For a liquidlike sample and temperatures close to 300 K, Eq. (1) is simplified considering a fast motion dynamics, where $\omega_s\tau_c \ll 1$, and can be written as

$$\frac{1}{T_2} \simeq \left(\frac{\mu_0}{4\pi}\right)^2 \hbar^2 \frac{\gamma_I^2\gamma_S^2}{r^6}\tau_c, \tag{2}$$

where τ_c is the correlation time of the motion. In the case of the homonuclear interaction, the expression for T_2 can be written as [18]

$$\frac{1}{T_2} = \frac{I(I+1)}{r^6}\left(\frac{\mu_0\hbar\gamma_I^2}{4\pi}\right)^2\left[\frac{3}{8}\mathcal{J}_0(0)+\frac{15}{4}\mathcal{J}_1(\omega_I)+\frac{3}{8}\mathcal{J}_2(2\omega_I)\right]. \tag{3}$$

By assuming similar dynamic condition for both homo and heteronuclear interactions, the homo and heteronuclear contributions to T_2 is related to the density of spins in the vicinity of the observed resonant nuclei. In fact if we concentrate the observation in ^{23}Na NMR nuclei, which are essentially located at the surface of micelles, then T_2 measures the spin density in the neighborhood of the surface. Of course, if there are different spin densities in the micellar surface, then it should be expected that this fact will be reflected in a dispersion in the T_2 relaxation profile. So, we can assign the local exponential decay amplitude of each compo-

nent of the T_2 profiles to different regions of the micellar surfaces, with different spin densities. It is important to stress that eventual orientational fluctuations of micelles *do not average* the dispersion in the T_2 relaxation profile. In other words, if anisometric micelles in an isotropic phase have three different regions with different spin densities (e.g., surfaces with different curvature radii), three peaks appear in the T_2-dispersion measurement.

C. Relaxation data analysis

The NMR ^{23}Na signal often shows multiexponential decays of the magnetization. These decay, together with the assumption that the dynamics of ^{23}Na are the same in all the micelles, constitute a map of the average distance between the ^{23}Na nuclei in the different micellar surroundings. These studies involve a detailed analysis of the distribution of T_2 by means of an algorithm based on a regularized least squares fit [19–23] of the experimental data by a sum of decaying exponentials. The fitting function is chosen as a linear combination, with non-negative coefficients $(C_j, 1 \leqslant j \leqslant M)$, of a finite set of M decaying exponentials with preestablished time constants. There is a unique solution such that the averaged sum of the squares (SQ) of the fitting errors is a minimum, and the constraints to be satisfied may be written as

$$\frac{\partial (SQ)}{\partial C_j} = 0 \quad \text{if } C_j > 0,$$

$$\frac{\partial (SQ)}{\partial C_j} \geqslant 0 \quad \text{if } C_j = 0.$$

It is not known beforehand which coefficients are positive.

Due to the weak linear independence of the exponential function, the fitting problem is an ill-defined one. This fact is reflected in strong oscillations in the spectral coefficients distribution. To cope with this situation, regularization is required. Of the various regularizations tried, the one producing the best results is that which accounts for the peak curvatures, by adding to SQ a term of the form

$$S_\theta = \frac{\theta}{M} \sum (C_{j-1} - 2C_j + C_{j+1}),$$

where θ is an external introduced *regularizing parameter*. S_θ plus the averaged sum of the squares is then minimized to obtain C_j''s.

Let us discuss in greater detail the association we will make between the amplitude of T_2 and the surface curvature of the micelles. In the neighborhood of the micellar surface (i.e., from the surface towards the bulk) an electric double layer constituted mainly by the $^{23}Na^+$ counterions is present. This layer involves the micelle and screens the negative charge of the ionized SDS molecules which constitute the micelle. In the case of ternary mixtures, it was shown that alcohol molecules are preferentially located in the flat parts of the micelle; however, to the best of our knowledge, this result has not yet been quantified. However, neutron results seem to indicate that alcohol molecules are not homogeneously distributed (mostly) in the flatter part of the micelle but segregate from the soap molecules, concentrating in the middle of the flatter surface. The amount (in mol) of alcohol with respect to the SDS in the ternary mixtures investigated in this work is defined by the parameter M_d, which varies in the interval $0.2 \leqslant M_d \leqslant 0.4$. As some of the alcohol molecules are also present in the curved surfaces of the micelle, it is reasonable to assume that the ^{23}Na nuclei interdistances are influenced (in the same sense) in both (flatter and curved) micellar surfaces by the alcohol molecules presence. In these alcohol concentrations, and taking into account neutrons' results, we do not expect that the ^{23}Na nuclei interdistances (present in the electric double layer) in the different micellar surfaces will be drastically modified in the sense that it would promote a larger ^{23}Na nuclei interdistances in the flatter surface and a smaller in the curved surfaces. We will return to this point later on during the results discussion.

III. RESULTS AND DISCUSSION

A. Binary mixture

Figure 1 shows the sodium T_2 measurements (in the isotropic phase $300 \leqslant T \leqslant 306$ K) of the binary mixture of sodium dodecyl sulfate and water. As discussed in the Introduction section, micelles in this mixture are expected to be spherical. Figure 1(a) shows the typical T_2-dispersion curve, which can be fitted by a single exponential decaying function. We verified that, increasing the number of exponentials in the fit of the magnetization decay, the χ^2 (which informs about the fit quality) does not significantly improves and the coefficients of the second, third, and so on exponentials are ~ 0 (i.e., $\leqslant$ than the coefficient of the first exponential). Figure 1(b) shows the linear behavior of T_2 with T. The T_2 peak integral (also named amplitude of the magnetization decay, shortly, *amplitude*), which is proportional to the number of ^{23}Na nuclei present in the sample, remains constant with temperature [Fig. 1(c)]. Following the arguments discussed just after Eq. (3) we can conclude that the spin density surrounding the ^{23}Na nucleus remains constant for all the sodium dodecyl sulfate molecules. In other words, this result is compatible with a model which assumes spherical micelles (only one radius of curvature) in this isotropic phase. The linear increasing of T_2 as a function of temperature [Fig. 1(b)] can be interpreted as a consequence of the increasing of the ^{23}Na-^{23}Na distance, due to the augmentation of the micellar radius with temperature. The surface per polar head increases with increasing temperature. One can, in this way, observe through the T_2-dispersion profile, the expansion of the micellar volume. The constant amplitude of the magnetization decay is also compatible with the above described model, showing that all ^{23}Na nuclei decays with the same T_2.

B. Ternary mixture

The T_2-dispersion measurements in the ternary mixtures with decanol concentrations $M_d = 0.2$, 0.31, 0.33 and 0.4 are shown in Figs. 2–5, respectively. The temperature evolution of the T_2 dispersion, with different values of M_d, are depicted in Figs. 2(a), 3(a), 4(a), and 5(a). The magnetization decay

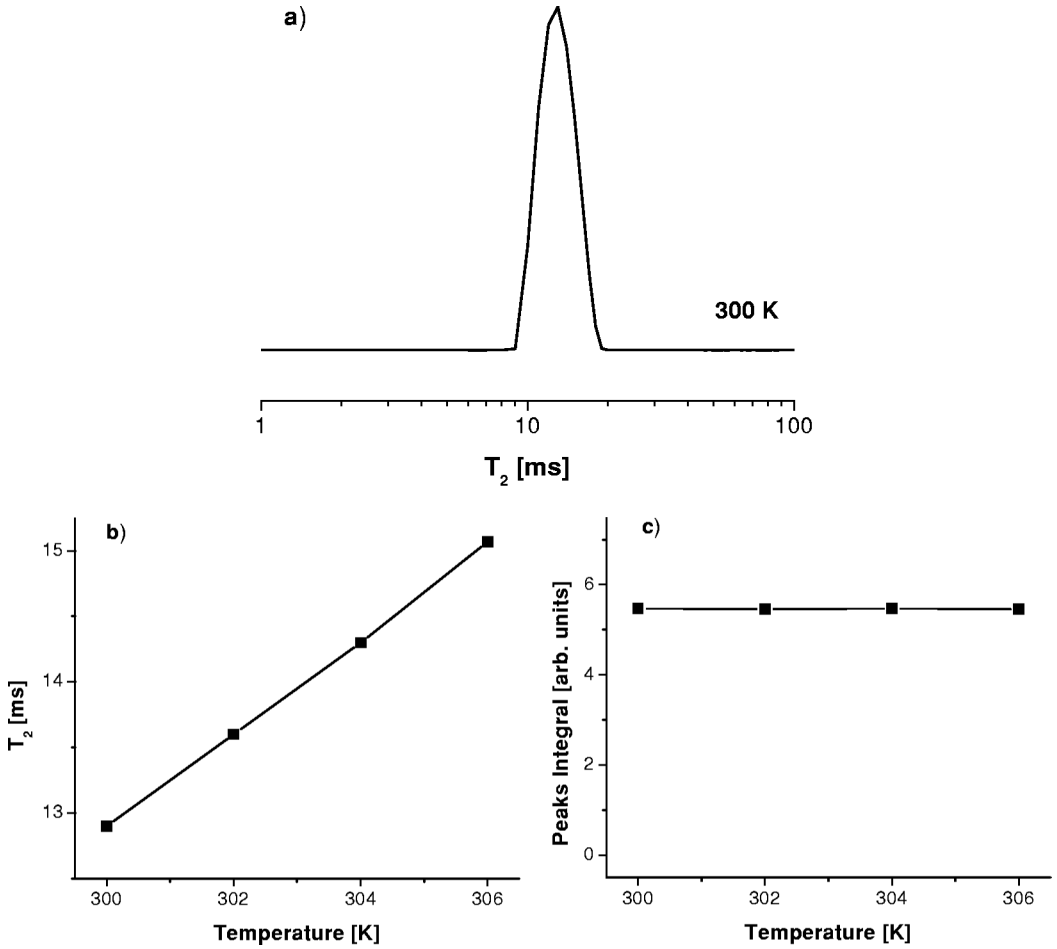

FIG. 1. (a) ^{23}Na NMR T_2-dispersion profile of the binary mixture of sodium dodecyl sulfate and water, isotropic phase; (b) T_2 as a function of temperature, sample in the isotropic phase; (c) T_2 amplitude as a function of temperature.

can be well described by three exponentials in the whole measured temperature range: (i) a first peak at low T_2 with a decay time constant below 2 ms, which cannot be adequately resolved by our experiment; (ii) a second intense peak centered in the range 5–10 ms; and (iii) a third one of, smaller amplitude, with T_2 higher than 10 ms. This general scheme is observed in both N_C and N_D uniaxial phases. As this is a crucial point of our analysis, let us discuss in more details the criterion used to conclude that the magnetization decay can be well described by three exponentials. Initially we verified that using a single exponential the fit quality is poor (large χ^2). Increasing the number of exponentials up to three, the fit quality approaches that of the single exponential fit obtained in the binary mixture. Increasing further the number of exponentials, the χ^2 does not significantly improves and the coefficients of the 4nd, 5rd and so on exponentials are ~ 0 (i.e., $\ll$ than the coefficients of the 1st, 2nd and 3rd exponentials).

At this point we can come back to the discussion about the influence of the alcohol molecules in the ^{23}Na nuclei interdistances. Comparing the values of T_2 obtained in the binary mixture (where only a curved surface is present in micelles) with those of the ternary mixtures we see that in all the cases there is a peak corresponding to $10 \lesssim T_2 \lesssim 30$ ms. Considering the amount of alcohol molecules present in the different mixtures and their location in micelles it seems reasonable to associate this peak (also in ternary mixtures) to the larger ^{23}Na nuclei interdistances, corresponding to curved surfaces. At the alcohol molecules concentration used, it seems unlike to attribute this peak (in ternary mixtures) to flatter surfaces where the ^{23}Na nuclei are moved away from each other due to the alcohol presence. Correspondingly, the other peaks observed in the ternary mixtures results (not observed in the binary mixture), particularly that at $1 \lesssim T_2 \lesssim 5$ ms, which is one order of magnitude smaller than that corresponding to the curved surfaces, should not correspond to a curved surfaces, with or without alcohol molecules.

The presence of three T_2' s in all the investigated temperature range can be interpreted, in our framework, as the indication that three spin densities coexist, *independently* of the uniaxial N_C or N_D phases. Each spin density is associated to different curvature radius in the micelle's surface. Let us discuss this aspect in more details. Assuming that micelles in the N_c and N_D phases are spherocylinders and disks, respectively, one should expect the presence of only two peaks in the T_2-dispersion measurements in each phase. In the case of spherocylindrical micelles (N_c phase), these two peaks correspond to the spin densities in the lateral surface and the end caps of micelles. In the case of disklike micelles (N_D phase), these two peaks correspond to the spin densities in the lateral

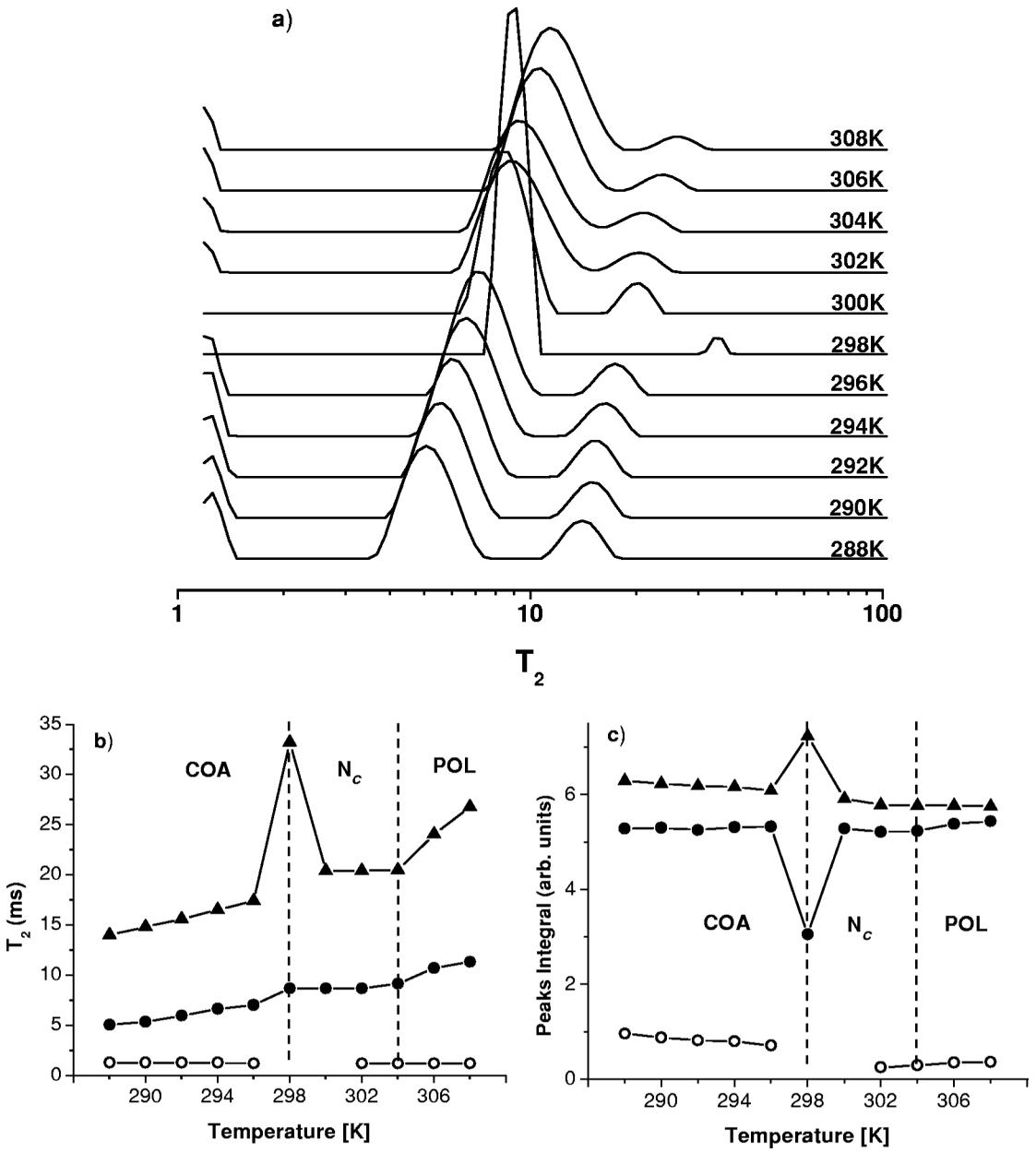

FIG. 2. (a) Experimental T_2 profile in the ternary mixture of SDS, decanol, and water, sample NC1, at different temperatures. (b) T_2 as a function of temperature, (◦) first peak, (•) second peak, (▲) third peak; (c) T_2 amplitude as a function of temperature, (◦) first peak, (•) second peak, (▲) third peak.

curved surface (half torus around the disc) and the flat top and bottom surfaces of micelles. On the other hand, a sketch of an intrinsically biaxial micelle (as proposed in the MIBM for the uniaxial and biaxial phases) is an ellipsoid with three different semiaxes. Figure 6 sketches this micelle, identifying the three different curved surfaces which should originate the peaks in the T_2-dispersion measurements. The numbers 1, 2, and 3 in the Fig. 6 are related to the origin of the first, second and third peaks in the T_2-dispersion measurements, respectively.

In Figs. 2(b) and 2(c) one can check the peak positions and amplitudes of sample NC1, respectively. T_2 of the second and third peaks increase with temperature [Fig. 2(b)] except at temperatures close to 298 K, where a strong increment of the high T_2 peak (third one) and the vanishing of the low component of the magnetization decay are shown. The amplitude of the third T_2 peak [Fig. 2(c)] also presents a maximum at that temperature. The maximum of T_2 and their respective amplitudes observed in temperatures around 298 K can be attributed to the COA-N_c phase transition. In addition, the increase of the slope of T_2 versus temperature at about 304 K should be identified to the N_C-POL transition [Fig. 2(b)]. Due to dynamic fluctuations of molecules in the vicinity of phase transitions, which promote fluctuations of the spectral densities [see Eqs. (1) and (3)], fluctuations in T_2 values are expected. This effect is seen in Figs. 2(b) and 2(c).

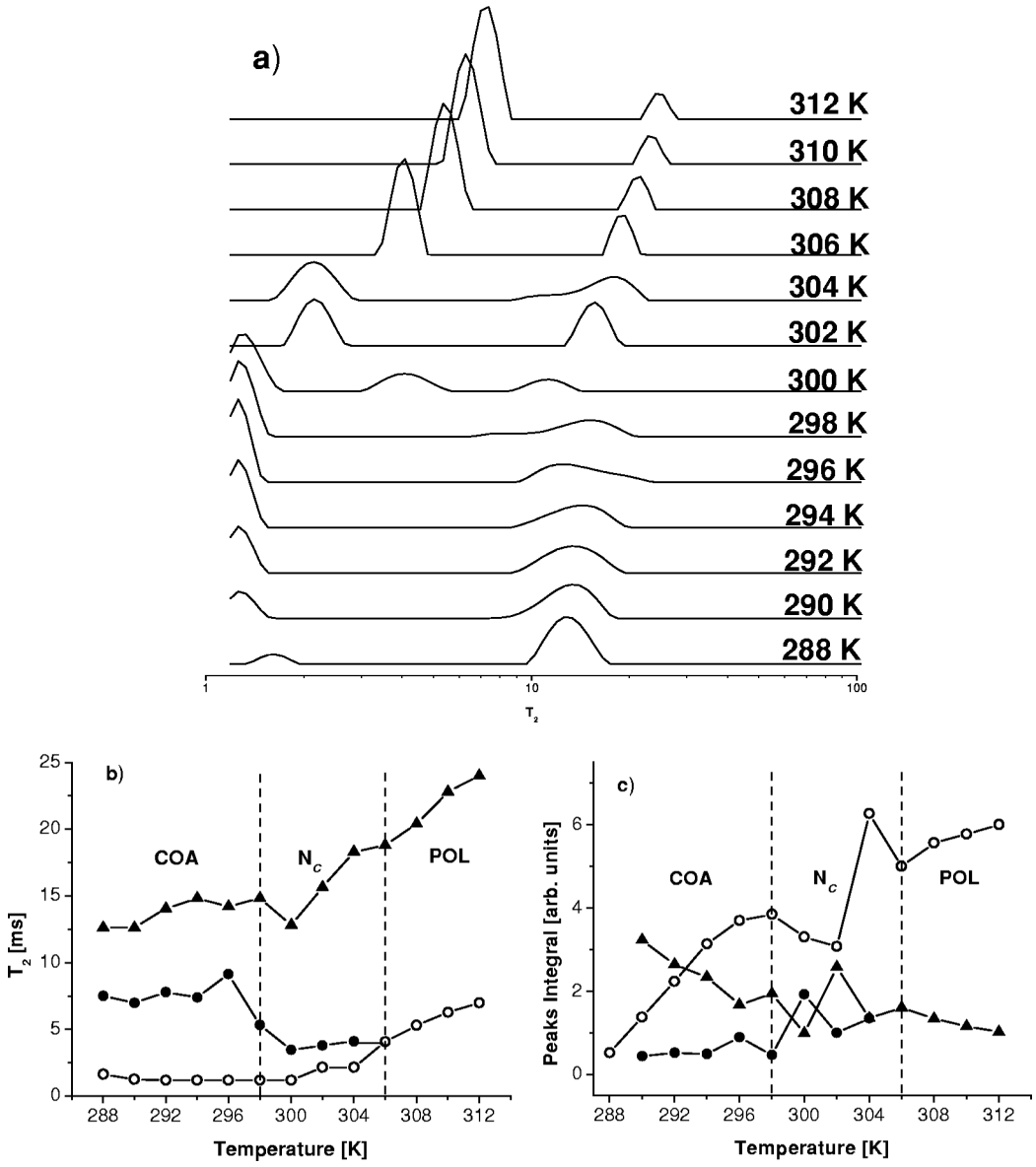

FIG. 3. (a) Experimental T_2 profile in the ternary mixture of SDS, decanol, and water, sample NC2. (b) T_2 as a function of temperature. (◦) first peak, (•) second peak, (▲) third peak; (c) T_2 amplitude as a function of temperature, (◦) first peak, (•) second peak, (▲) third peak.

Our results indicate that these spin densities do not significantly change in all the COA, N_C and POL regions of the phase diagram.

The T_2 dispersion profile behavior [Figs. 3(a)–3(c)] in the sample with higher water concentration (M_d=0.31), named NC2, is essentially the same described above. In the COA phase domain, the second and third T_2 peaks are visually unresolved, but numerical fitting allows to calculate the values plotted in Figs. 3(b) and 3(c). The transition between the N_C phase and POL occurs in 306 K, signed by a change in the T_2 versus temperature curve slope of both second and third peaks. The amplitude of the first T_2 peak increases with temperature until $T\sim 298$ K while, in the same T-range, the amplitude of the third peak decreases. The amplitude of the second T_2 peak remain barely constant at $T<298$ K.

Similar behaviors were observed at a higher water concentration sample (M_d=0.33), named NC3, as depicted in the Figs. 4(a)–4(c). In this sample the N_C-POL transition occurs at $T\sim 296$ K.

In the case of sample with M_d=0.4, named ND 1, the N_D phase domain is limited at low temperature (at ~292 K) by a coagel phase and at high temperature (at ~296 K) by a POL domain. Figure 5 shows the experimental T_2 dispersion measured in this sample.

As a remark, it can be observed that the behavior of the T_2 profiles of the NCi (i=1, 2, and 3) and ND1 samples closely match. This means that in the N_C and N_D phases, the spin densities in the micellar surfaces are similar, which is consistent with the MIBM.

Let us analyze the amplitude of the first T_2 peak (associated to the flattest surface of micelles) as a function of $M_d(0.2\leqslant M_d\leqslant 0.4)$ at a fixed temperature, in the nematic phase domain. We observe that the amplitude of this peak increase with M_d. In the N_D phase, its value became ~3

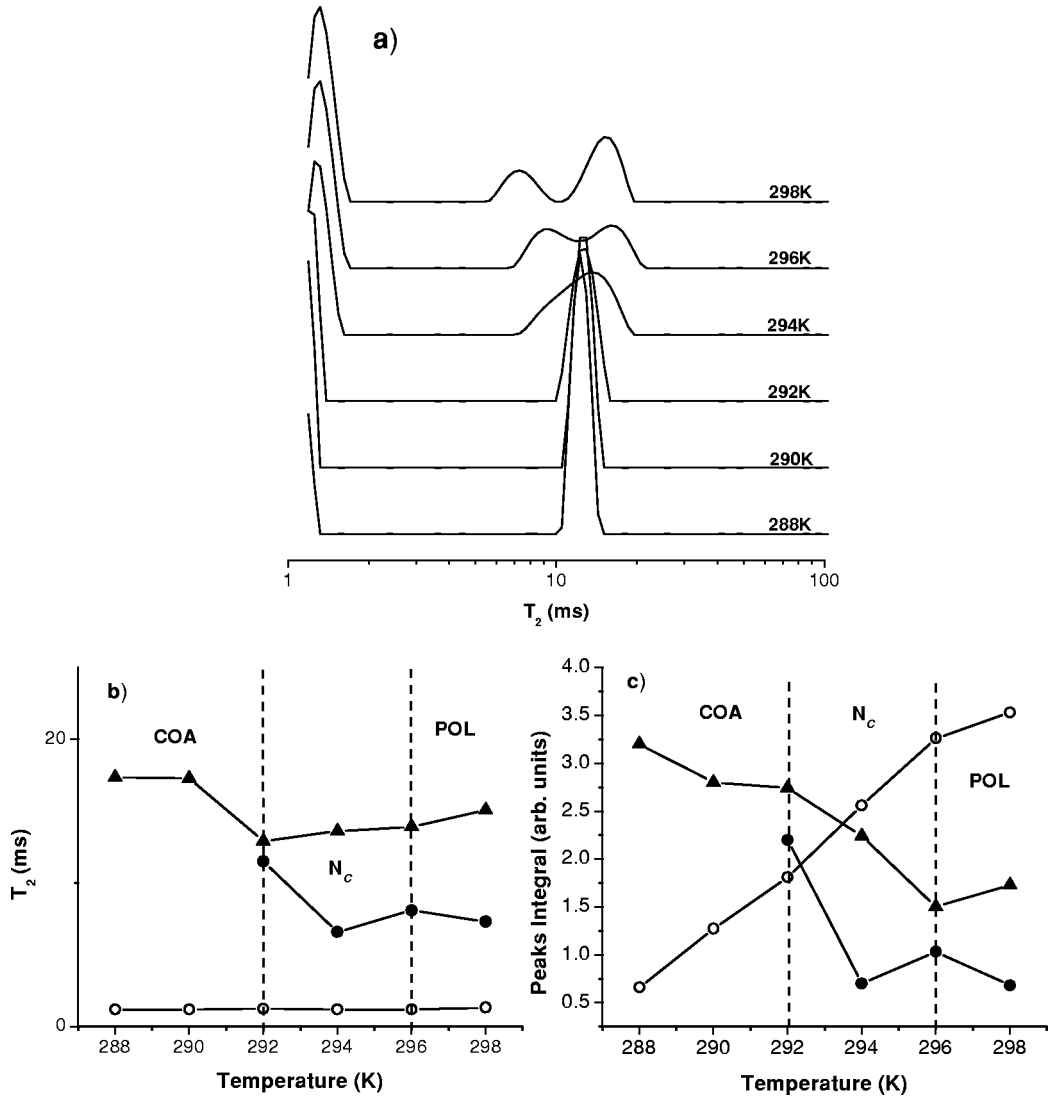

FIG. 4. (a) Experimental T_2 profile in the ternary mixture of SDS, decanol, and water, sample NC3. (b) T_2 as a function of temperature. (◦) first peak, (•) second peak, (▲) third peak; (c) (T_2) amplitude as a function of temperature, (◦) first peak, (•) second peak, (▲) third peak.

times larger than that in the N_C phase. In our framework, small values of T_2 are associated to small ^{23}Na-^{23}Na distances, i.e., flatter surfaces. Microscopically, the presence of larger T_2 amplitude encountered in the N_D phase indicate the presence of larger flat surfaces in micelles in this phase, with respect to those in the N_C phases. This fact is compatible with the MIBM which assumes that the micellar dimensions continuously change with temperature across the phase transitions and orientational fluctuations originate macroscopically the different nematic phases. In the N_D phase orientational fluctuations which degenerate the axis perpendicular to the biggest micellar surface take place. These fluctuations are favored when micelles have larger flat surfaces with respect to curved surfaces. In both nematic phases the first peak (low T_2) position remains practically temperature independent, even in the N_D phase. Taking into account that the values of T_2 of the first peak are almost independent of temperature and those of the third peak depend on T, it is reasonable to conclude that amphiphilic molecules located in the curved loci of micelles experience a bigger temperature variation of their surface per polar head with respect to molecules placed in the flatter part of micelles.

The peak in the dispersion profile, located approximately at $T_2=5$ ms (second peak), is associated with regions of the micellar surface presenting intermediate curvature radii.

Let us analyze now the high T_2 peak (the third one), which is located in the range between 10 and 12 ms. This peak should be associated to the largest distances between ^{23}Na nuclei and, consequently, to the shortest curvature radii of the micellar surfaces (where the ^{23}Na nuclei are located). The values of T_2 in the N_D phase are similar to those measured in the spherical micelles of the binary mixture. So, we can partially conclude that the shortest curvature radius in the N_D phase (ternary mixture) is similar (in both absolute value and thermal behavior) to the mean radius of the spherical micelles in the binary mixture. The situation is rather different in the N_C phase. Comparatively higher T_2 and thermal expansion coefficients have been observed in the samples NCi($i=1,2$ and 3). These higher T_2 values correspond to smaller curvature radii in micelles.

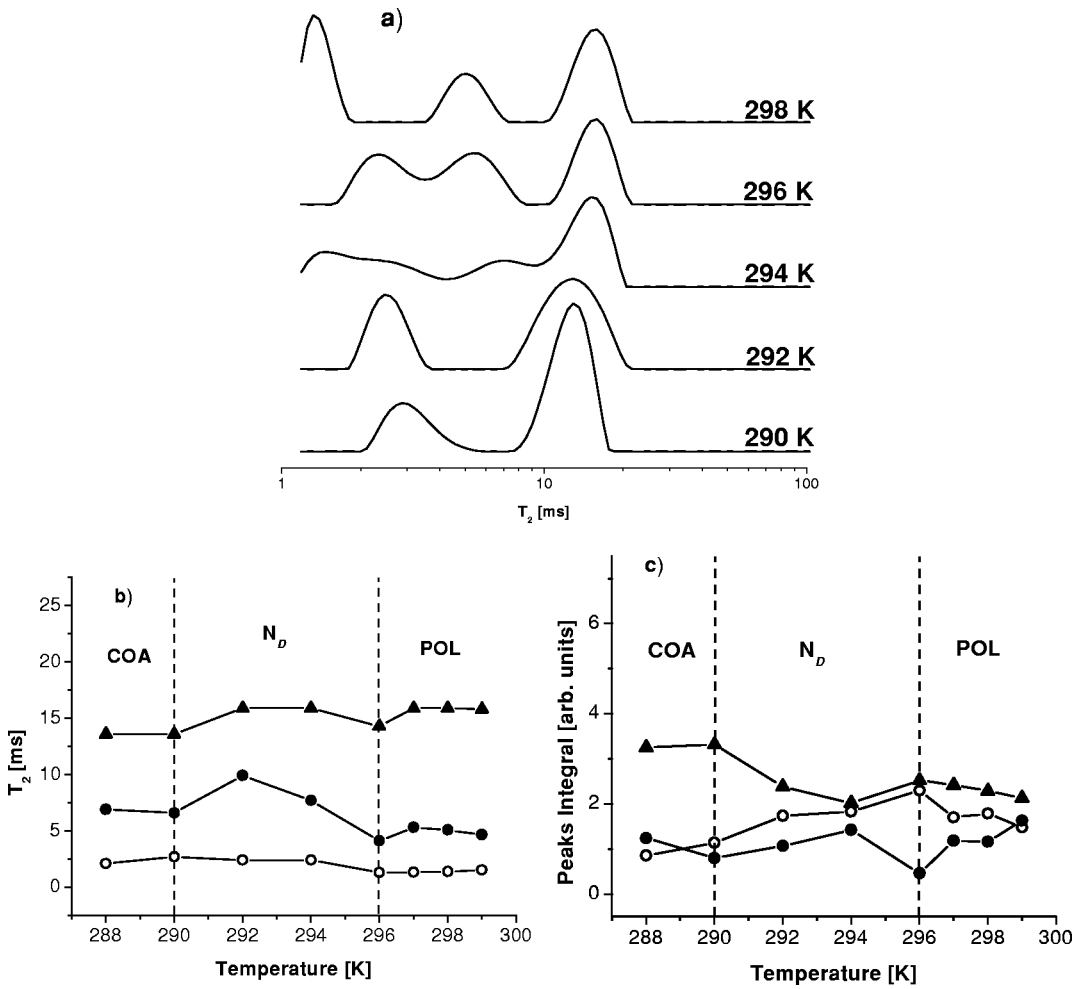

FIG. 5. (a) Experimental T_2 profile in the ternary mixture of SDS, decanol, and water, sample ND1. (b) T_2 as a function of temperature, (◦) first peak, (•) second peak, (▲) third peak; (c) T_2 amplitude as a function of temperature, (◦) first peak, (•) second peak, (▲) third peak.

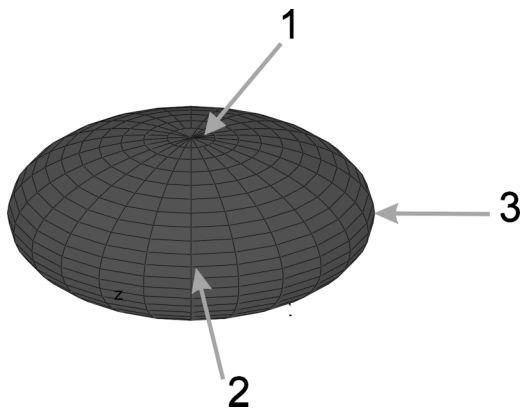

FIG. 6. Schematic representation of an intrinsically biaxial micelle (ellipsoid with three different semiaxes). The smallest distances between ^{23}Na nuclei correspond to the flat surface (region 1); the largest distances between ^{23}Na nuclei correspond to the most curved surfaces (region 3); intermediary distances between ^{23}Na nuclei correspond to intermediary curvature regions 2.

IV. CONCLUSIONS

In this work we developed a method by which to study the shape of micellar aggregates based on the measurements of the NMR spin-spin relaxation dispersion profiles. The basic idea is that, at equally dynamic behavior, the spin-spin interactions essentially depends on the distance between the studied NMR nuclei and its surrounding spins. In this framework, it is possible to associate flat micellar surfaces with short distances between ^{23}Na nuclei, and consequently shortest T_2's.

This picture is corroborated by the study of the T_2-dispersion profile carried out in the binary sodium dodecyl sulfate–water mixture. The magnetization decay is well described by a single exponential, as expected for spherically shaped micelles. From the measurements of T_2 at different temperatures (in the isotropic phase), we observed that the thermal expansion of the micellar dimension is nicely described by the linear increment of the single T_2 with temperature.

The analysis of the T_2 dispersion profiles in both the uniaxial nematic calamitic and discotic phases indicates that highly symmetrical micellar shapes like spherocylinders and disks do not account for the experimental results obtained in

our experiments, where three peaks are present. Our results can be interpreted in terms of the model of intrinsically biaxial micelles in all the nematic phases. The micellar dimensions present continuous changes in their dimensions as a function of external variables like temperature and relative concentrations of the mixture components.

Moreover, the T_2 dispersion profile analysis of a single nucleus located preferentially in the head region of the amphiphilic molecules is a useful tool to parametrize some properties of the shape of the micellar surface. Possible extension of the proposed analysis method to more complex structures like sponge phase, membranes, etc., is a matter for future studies.

ACKNOWLEDGMENTS

We are thankful for the financial support from Argentina, to the CONICET and CONICOR agencies, and from Brazil, to the FAPESP, PRONEX and CNPq agencies.

[1] C. Tanford, in *The Hydrophobic Effect: Formation of Micelles and Biological Membranes* (Wiley, New York, 1980).
[2] K. D. Lawson and T. J. Flaut, J. Am. Chem. Soc. **89**, 5489 (1967); P. J. Black, K. D. Lawson, and T. J. Flaut, Mol. Cryst. Liq. Cryst. **7**, 201 (1969).
[3] J. Charvolin, A. M. Levelut, and E. T. Samulski, J. Phys. (France) Lett. **40**, L-587 (1979).
[4] L. J. Yu and A. Saupe, Phys. Rev. Lett. **45**, 1000 (1980).
[5] Y. Galerne, A. M. Figueiredo Neto, and L. Liébert, J. Chem. Phys. **87**, 1851 (1987).
[6] F. Fujiwara, L. W. Reeves, M. Suzuki, and J. A. Vanin, in *Solution Chemistry of Surfactants*, edited by K. L. Mittal (Plenum, New York, 1979), Vol. 1.
[7] Y. Hendrikx, J. Charvolin, and M. Rawiso, Phys. Rev. B **33**, 3534 (1986).
[8] P. O. Quist, B. Halle, and I. Furó, J. Chem. Phys. **96**, 3875 (1992).
[9] N. Boden, S. A. Corne, M. C. Holmes, P. H. Jackson, D. Parker, and K. Wolley, J. Phys. (France) **47**, 2135 (1986).
[10] P. Photinos and A. Saupe, Phys. Rev. A **43**, 2890 (1991).
[11] M. C. Holmes, J. Charvolin, and D. J. Reynolds, Liq. Cryst. **3**, 1147 (1988).
[12] L. Q. Amaral, C. A. Pimentel, M. R. Tavares, and J. A. Vanin, J. Chem. Phys. **71**, 2940 (1979).
[13] M. J. Sammon, J. A. N. Zasadzinski, and M. R. Kuzma, Phys. Rev. Lett. **57**, 2834 (1986).
[14] K. R. Browenstein and C. E. Tarr, Phys. Rev. A **19**, 2446 (1979).
[15] L. Q. Amaral and M. E. Marcondes Helene, J. Chem. Phys. **92**, 6094 (1988).
[16] E. Fukushima and S. B. W. Roeder, *Experimental Pulse NMR* (Addison-Welsey, Redwood City, CA, 1981).
[17] S. Meiboom and D. Gill, Rev. Sci. Instrum. **29**, 688 (1958).
[18] R. Kimmich, *NMR Tomography, Diffusimetry, and Relaxometry* (Springer-Verlag, Berlin, 1997).
[19] J. P. Butler, J. A. Reeds, and S. V. Dawson, SIAM (Soc. Ind. Appl. Math.) J. Numer. Anal. **381**, 18 (1981).
[20] D. P. Gallegos and D. M. Smith, J. Colloid Interface Sci. **143**, 122 (1988).
[21] K. P. Whittall and A. L. MacKay, J. Magn. Reson. **134**, 84 (1998).
[22] S. Davies and K. J. Packer, J. Appl. Phys. **3163**, 67 (1990).
[23] S. Davies, M. Z. Kalam, K. J. Packer, and F. O. Zelaya, J. Appl. Phys. **3171**, 67 (1990).